STRESSES IN CONCRETE PAVEMENT SLABS

By M G Spangler

Associate Structural Engineer, Iowa Engineering Experiment Station,

and

Frank E Lightburn

Assistant Professor of Theoretical and Applied Mechanics, Iowa State College

SYNOPSIS

The Iowa Engineering Experiment Station has been conducting a research project for several years on the subject of stresses in concrete pavement slabs This paper is the second progress report on the project and will give the results of some extensive strain measurements from which the magnitude and direction of the principal stresses have been determined at a large number of points in the vicinity of loads applied at a corner of two full scale model slabs

The subgrade reaction pressures and deflections of one of the slabs have been measured at a number of points over the corner region and the ratio between pressure and deflection at each of the points determined These studies show that, for this slab, the ratio was constant at each point within the range of loads applied, but was not the same constant at all points since it varied with the distance of a point from the corner The values of the ratio varied from about 300 lb per sq in per in at the corner to about 75 lb per sq in per in at distances of 4½ ft from the corner The use of a uniform value of the ratio appears to be a justifiable assumption for analytical solutions, however, since average normal stresses calculated by formulas using a uniform value of 200 checked closely with average normal stresses calculated from measured strains, and also those calculated from measured pressures

The analytical determination of stresses in a concrete pavement slab when treated as an elastic plate on an elastic foundation involves a ratio between the subgrade pressure and the vertical deflection of the slab, which is usually assumed to be a constant of the same value at each point The researches of Goldbeck (1)[a] and others have shown that when loads are applied to an earth mass, the relationship between pressure and vertical movement is not a constant, but is a function of the area over which the load is applied Although a pavement slab is not a uniformly loaded area in the sense investigated by Goldbeck, it has seemed probable that the subgrade pressure may be affected by the same principle, and that the pressure at any point may be a function of position as well as deflection of the slab at that point Westergaard recognized and discussed this question in his published analysis of pavement slabs in 1925 (8)

[a] Figures in parentheses refer to list of references at end

This paper is the second progress report on some studies being conducted by the Iowa Engineering Experiment Station on the subject of stresses in concrete pavement slabs It gives the results of measurements of subgrade pressures, deflections, and principal stresses on two full scale model concrete slabs which have been studied during the past two years In both cases the measurements have been confined to the region adjacent to a load concentrated over a small area and applied at a corner of the slab The slabs have been numbered 3 and 4 for reference

The subgrade pressures were measured by means of Goldbeck pressure cells cast in the concrete In slab No 3, an attempt to measure subgrade pressure was wholly unsuccessful due, apparently, to the fact that no provision was made for initial adjustment of the pressure between the cells and the subgrade

For slab No 4, a device was designed and installed which permitted adjustment of the initial subgrade pressure

With this adjustment the cells yielded results which were remarkably consistent for measurements of this type

Deflections of the slabs were measured by means of 0 0001-in Federal dials mounted on an I-beam framework supported independently of the slabs

Strains in the top surface of the slab were measured by means of pairs of optical lever extensometers of the type described by Spangler (6), except that the fixed knife edge of each extensometer was made adjustable, a modification which greatly facilitated the initial adjustment of the mirrors The surface strains were measured along three gage lines at each of a large number of points distributed over the corner region The principal strains and stresses at each point were calculated from these tri-axial strain readings

All of the experimental slabs were located in the basement of the Experiment Station Laboratory where there was little variation in temperature They were constructed on a yellow clay subgrade which was confined in a box 14 ft square and 2 ft deep The clay was placed and hand tamped in layers of about 5 in No attempt was made to determine the properties or moisture content of the clay, although provision was made to hold the moisture content as nearly constant as possible during the test period Slab No 3 was constructed on a subgrade which had been in place for three years, and it had been allowed to dry out until it was unduly stiff Therefore it was decided that the clay should be taken out, moistened and retamped for the subgrade of slab No 4

TABLE 1

	Slab No 3	Slab No 4
Constructed	June 18, 1935	June 24, 1936
Tested	7/5/35 to 9/20/35	7/15/36 to 8/15/36 1/9/37 to 2/23/37
Size	10 x 12 ft	12 x 12 ft
Thickness	6 in	6 in
Reinforcing	None	None
Cement	High early strength	High early strength
Coarse aggregate	Limsetone	Limestone
Mix by weight	1 4 4	1 4 4
Water-cement ratio by weight	0 80	0 75
Control specimens	Cylinders and beams	Cylinders and beams
Curing	Under moist burlap	Under moist burlap
Average Properties at Time of Test		
Compressive strength, lb per sq in	3,300	4,700
Modulus of rupture, lb per sq in	520	680
Modulus of elasticity, lb per sq in	2,770,000	4,000,000
Poisson's ratio	0 20	0 25

Table 1 gives some of the more pertinent information on the third and fourth slabs

To avoid confusion and misinterpretation, a number of terms used in this paper are defined as follows

Principal stresses are the stresses at a given point which occur at right angles to planes on which the shearing stress is zero One of these is the maximum and the other the minimum stress at the point

Principal strains are the strains in the direction of the principal stresses and are the maximum and minimum strains at a given point

Rosette strains are the strains measured on three different gage lines passing through a given point

Radial strain is the strain along a line which passes through the corner

Normal stress is the stress at a given point in the slab which is at right angles to a line perpendicular to the corner bisector, or in other words a stress which is parallel to the corner bisector This is the stress which Westergaard (8) assumed to be uniformly distributed over a line perpendicular to the corner bisector

Average normal stress is the stress which is the average ordinate of a curve showing the actual distribution of the normal stress over a line perpendicular to the corner bisector

Apparent stress is a factitious stress which is obtained by multiplying the unit radial strain by the modulus of elasticity

In this paper the terms stress and strain are used to denote unit stress and unit strain unless otherwise noted

STRESS MEASUREMENTS ON SLAB 4 [b]

In order to determine completely the stresses at a point in the surface of a slab it is necessary to measure strains on three different gage lines through the given point The points on slab No 4 at which rosette strain readings were taken are shown in Figure 1 These points will be designated by giving the number and letter of the lines intersecting at the point as A-1, B-7, etc The gages had a length of 3 in and they were centered over the points with the exception of the points at the edge, where they were placed as nearly over the points as the proximity to the edge would permit

Load was applied in increments, and strain readings taken at 3,000, 4,000, and 5,000 lb Within the loading range the strain readings at a given point were directly proportional to the load The optical lever extensometers used to measure these strains were arranged in pairs on each gage length in order that the

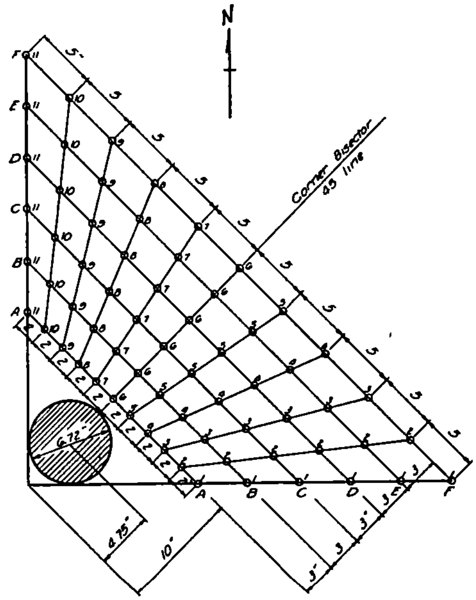

Figure 1. Arrangement of Points for Rosette Strain Readings Slab No 4

rotation of the mirrors caused by the change in slope of the slab as it deflected under load could be eliminated The mirrors of the two extensometers of a pair were arranged to rotate in opposite directions due to surface strains, and since the change in slope caused them to rotate in the same direction, the algebraic average of the scale differences for a pair of extensometers gave the net mirror rotation due to surface strain only The loading arrangement and some of the extensometers may be seen in Figure 2

After the scale differences were taken

[b] This discussion of stresses in slab No 4 is based on data, the greater part of which was obtained by W E Hitchcock (2) and was the basis for his thesis for the degree, Master of Science, granted him by Iowa State College in June 1937

TABLE 2

SAMPLE DATA

Slab No. 4—Diameter of Loading Area, 6.72 in.—Load, 5,000 lb. Line F

Point No.	Measured unit strains x 10^{-6}			Calculated unit strains x 10^{-6}		Direction of maximum principal strain and stress*	Calculated stresses lb. per sq. in.		
	45° to Line F*	90° to Line F*	135° to Line F*	Maximum principal strain	Minimum principal strain		Maximum principal stress	Minimum principal stress	Normal stress
	(1)	(2)	(3)	(4)	(5)	(6)	(7)	(8)	(9)
1	− 5.2	+44.0[2]	+45.8	+54.8	−14.7	113.8°	+217	− 4.0	+181
2	− 5.8	+53.0	+41.6	+60.1	−24.2	107.2°	+230	−39.2	+207
3	− 4.6	+54.1	+38.7	+60.0	−25.8	105.2°	+228	−46.1	+209
4	+ 4.1	+65.4	+35.3	+68.0	−28.7	99.5°	+259	−49.8	+252
5	+14.3	+70.2	+33.7	+71.4	−23.1	96.0°	+280	−22.2	+277
6	+23.4	+67.6	+32.8	+68.0	−11.9	90.0°	+277	−21.7	+277
7	+23.5	+69.1	+19.2	+69.1	−26.3	89.0°	+266	−38.4	+266
8	+37.5	+68.4	+ 9.4	+70.6	−23.8	81.5°	+276	−26.0	+269
9	+39.4	+70.3	− 5.8	+74.9	−41.3	78.5°	+275	−96.4	+261
10	−15.9[1]	+51.8	− 6.3	+59.7	−23.8	72.2°	+229	−37.9	+205
11	+43.5	+44.0[2]	− 8.3	+54.7	−19.4	67.9°	+212	−24.3	+179

Plus signs indicate tension, minus signs compression.

* Angles are measured clockwise from Line F (See Fig. 1).

[1] To avoid an obstruction in the line of sight this reading was taken along Line F instead of 45° to it.

[2] Values for points 1 and 11 in this column are extrapolated.

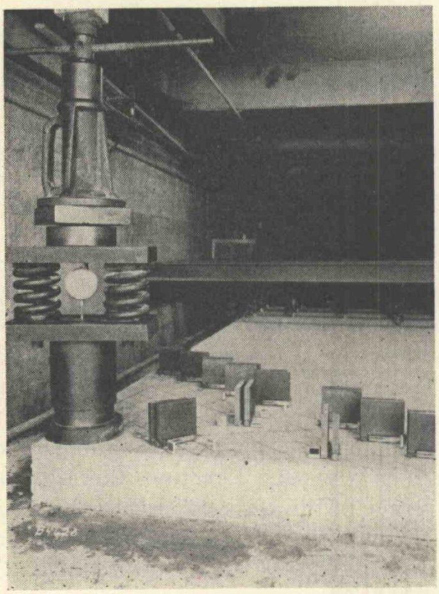

Figure 2. Loading Apparatus and Mirror Extensometers at S. W. Corner of Slab No. 4

and the algebraic average obtained they were converted into unit strains by the formula

$$\delta = \frac{SW}{2GD} \qquad (1)$$

in which

δ = unit strain.
S = algebraic average of scale differences.
W = height of the diamond knife edge.
G = gage length.
D = distance from mirror to scale.

Columns 1, 2, and 3 in Table 2 give unit strains at the various points on line F as calculated by this formula. These values are the average obtained by three separate loadings of the slab. Individual readings showed variations of about three to five percent from the mean in regions where the measured unit strains were 20 to 80 millionths. This range included the important strains In some cases the unit strains were below 10 millionths, a few even being less than 1 millionth These values approach the limit of precision of the extensometers which was about $1\frac{1}{2}$ millionths with the lengths of optical levers used Variations of individual readings in this last group ran as high as 20 percent of the mean

Due to a lack of understanding of the stress situation along the edge of the slab, strain readings were taken on only two gage lines at all of the edge points Later it was realized that strain measurements on three gage lines were necessary at edge points as well as interior points The approximate strain on a third gage line was obtained by extrapolating the curves on the strain readings on interior gage lines parallel to this third gage line As a check on this extrapolation the stresses normal to the edge were computed at each edge point and compared with the actual stress normal to the edge which is known to be zero The greatest stress normal to the edge computed in this manner was 17 percent and the average of all values was only 9 percent of the principal stress at the edge

Having these rosette strain measurements, the magnitude and direction of principal strains at each point may be obtained graphically by a method described and explained by Osgood and Sturm (5) A sample of this graphical construction has been carried out for point F-2 and is shown in Figure 3

The principal stresses shown in columns 7 and 8 were obtained from the principal strains by the equations

$$\sigma_{max} = \frac{E}{1-\mu^2}\,(\delta_{max}+\mu\delta_{min}) \,. \quad (2)$$

$$\sigma_{min} = \frac{E}{1-\mu^2}\,(\delta_{min}+\mu\delta_{max}) \quad . \quad (3)$$

where σ_{max} and σ_{min} are the maximum and minimum principal stresses respectively, δ_{max} and δ_{min} are the maximum and minimum principal strains Tensile strains are considered positive and compressive strains negative E is the modulus of elasticity and μ is Poisson's Ratio

The normal stresses shown in column 8 were determined from the principal stresses by the equation

$$\sigma_n = \frac{\sigma_{max}+\sigma_{min}}{2} + \frac{\sigma_{max}-\sigma_{min}}{2}\cos 2\theta \quad (4)$$

In this equation σ_n is the normal stress, σ_{max} and σ_{min} the maximum and minimum principal stresses respectively, tensile stresses are considered positive and com-

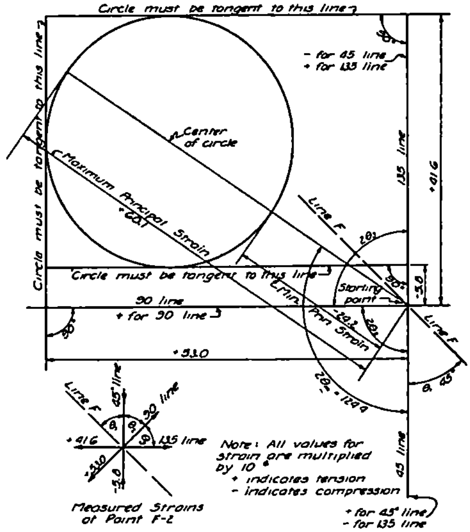

Figure 3 Graphical Construction for Obtaining Magnitude and Direction of Principal Strains from Rosette Strains

pressive stresses negative, and θ the angle between the direction of the maximum principal stress and the direction of the normal stress

These equations may be found in almost any textbook on Mechanics or Theory of Elasticity (7)

The magnitude and direction of the maximum principal stress at each of the 66 points are shown in Figure 4 It is of interest to note that the direction of this principal stress was approximately parallel to the corner bisector for almost all points It may be further noted that there is a comparatively large area in the vicinity of the corner over which the stress was fairly uniform This may also be seen in Figure 5 which is an iso-stress

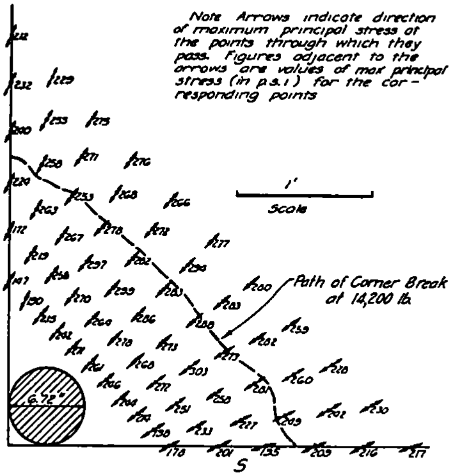

Figure 4 Magnitude and Direction of Maximum Principal Stresses Slab No 4, 5,000-Lb Load

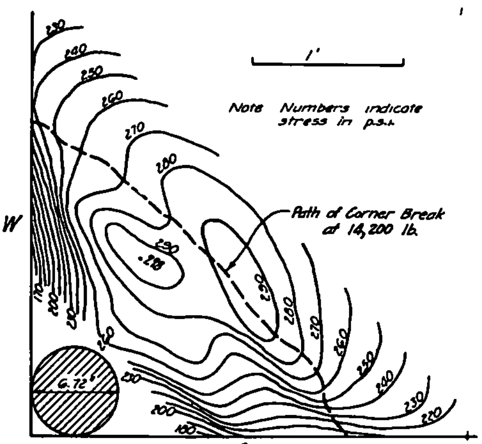

Figure 5 Iso-Stress Diagram for Maximum Principal Stresses, Slab No 4, 5,000-Lb Load

diagram for maximum principal stress, or in other words a stress contour diagram Data for this diagram were obtained by plotting the principal stresses against distance along the radial lines and drawing a smooth curve through the points. which. of course, has the effect of smoothing out the diagram In general, the principal stresses at points along the edges of the slab are about 20 to 40 percent less than the principal stresses along the corner bisector This situation is the reverse of that reported by Murphy (4) whose ana-

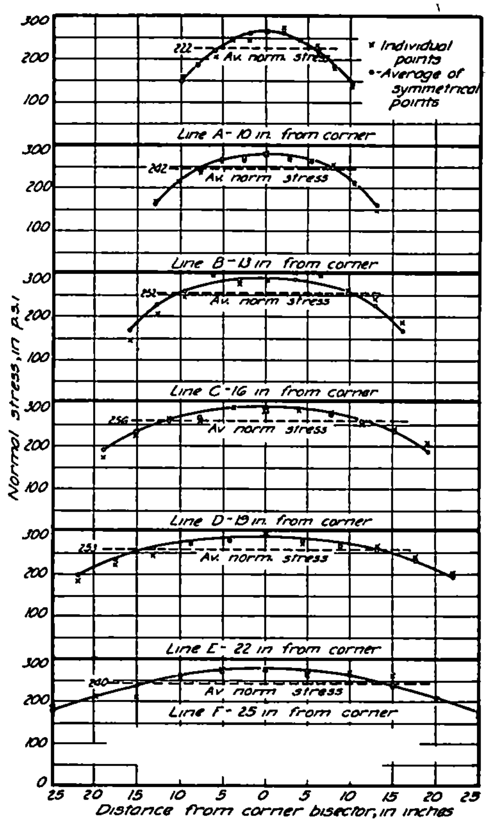

Figure 6 Distribution of Normal Stress Along Lines Perpendicular to Corner Bisector Slab No 4, 5,000-Lb Load

lytical solution yielded greater stresses at the edge than along the bisector

If the normal stresses, such as those in column 8 of Table 2, are plotted over the lines perpendicular to the corner bisector, the curves shown in Figure 6 are obtained The area under these curves divided by the length of the line over which the curve was plotted gives the average normal stress along that line

A planimeter was used to determine the areas

Since the direction of the maximum principal stresses at points on the corner bisector is parallel to the corner bisector due to symmetry about this line, the value of θ in equation 4 is zero Hence, for all points on the bisector, the normal stress is equal to the maximum principal stress

Consider a triangular section of the corner formed by the edges and one of the lines marked by letters (see Fig 1) There is a total bending moment acting on this section caused by the load and the subgrade reaction If this moment is assumed to be uniformly distributed over the width of the section, and a stress calculated from it, that stress will be what has been defined as the average normal stress This procedure was followed by Westergaard (8) in his analytical solution for the stress caused by corner loads and subsequently by Spangler (6) in deriving an equation for minimum probable stress

It can be seen from Figure 6 that the normal stress is not uniformly distributed over lines perpendicular to the corner bisector and that the maximum normal stress is 13 percent to 18 percent greater than the average normal stress depending upon the line considered Therefore, it would seem that if a stress is calculated from a total bending moment by assuming a uniform distribution of moment, approximately 15 percent should be added to that stress to get the maximum value

A comparison of experimental and analytical values of stress along the corner bisector is given in Figure 7 The apparent stress which is the radial unit strain times the modulus of elasticity is from 14 percent greater to 4 percent less than the maximum principal stress The minimum principal stress which is a compressive stress in the top surface gives an indication of the tensile stress which might be expected on the bottom of the slab These tensile stresses in the bottom surface were relatively small in this slab, but some studies by Lightburn (3) indicate that they may be of importance in some cases He investigated small rectangular plaster slabs, 9 in square and ½ in thick, under loads concentrated over a small area and supported on a rubber subgrade With certain loads at the corners of these slabs, he noted that the ma-

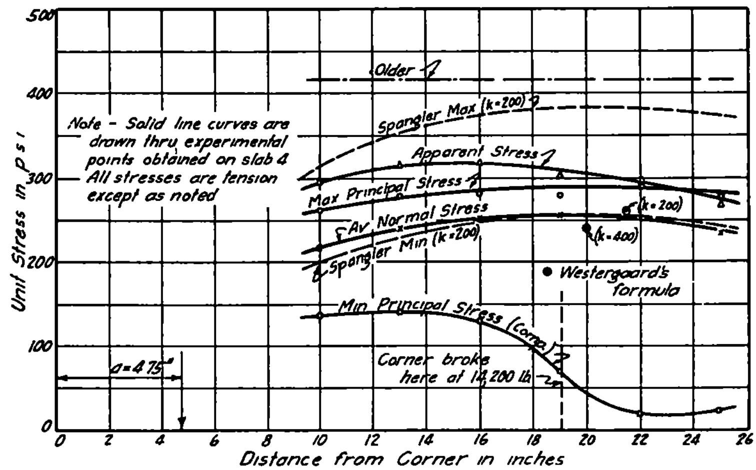

Figure 7 Comparative Values of Stresses Along the Corner Bisector, 5,000-Lb Load

terial failed along the corner bisector by tension in the bottom face before the ordinary corner break occurred

Older's equation (8) for the maximum stress in a slab gives values which are 46 percent greater than the highest experimental value obtained in these tests Assuming a value of 200 lb per sq in per in for the modulus of subgrade reaction, which should seem reasonable in the light of subsequent data, Westergaard's (8)

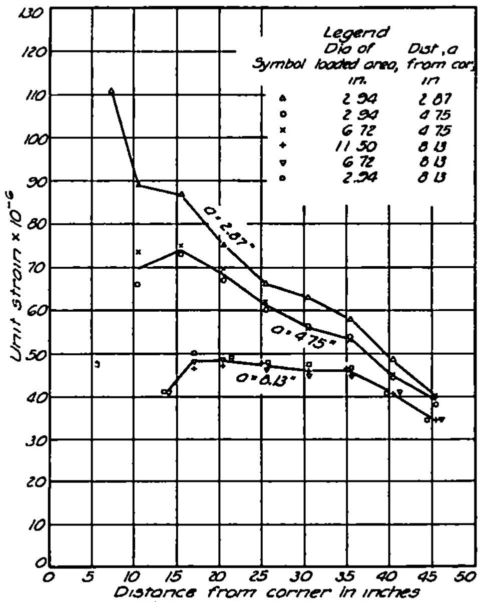

Figure 8 Variation in Radial Strain Along Corner Bisector Due to Size and Location of Loading Area, Slab No 4, 5,000-Lb Load

(9) expression gives a stress which is 10 percent less than the highest experimental value The two expressions for maximum and minimum probable stress suggested by Spangler (6) give results which are 33 percent higher and 14 percent lower, respectively, than the greatest experimental stress

The curves in Figure 8 indicate approximately the effect on stresses of the size and position of the loading area The curves show radial unit strain along the bisector which may be taken as approximately proportional to the stress along the bisector They indicate quite definitely that the stress is a function of the distance from the corner to the centroid of the load and that the stress is more or less independent of the size of the loaded area

After all the strain measurements were completed, a load was applied to the southwest corner of the slab until it broke The path of the corner break, which occurred at a load of 14,200 lb, is shown in Figures 4 and 5

STRESS MEASUREMENTS ON SLAB NO 3

The strain measurements and calculations of principal stresses were carried out on slab No 3 in exactly the same manner as for slab No 4, except that the 50 points at which rosette strains were measured were on only five radial lines passing through the corner These points covered a greater total area than on the later slab As a result of this distribution of points, there were rather wide areas in which no stress values were known and it was difficult to trace the iso-stress lines with certainty However, with certain trends definitely established as the result of the better distribution of points on slab No 4, the data for No 3 were interpreted with more confidence

The directions of the principal stresses were much like those shown for slab No 4, that is, they were approximately parallel to the corner bisector The magnitudes of the principal stresses for several different loading areas and positions of load are shown in the iso-stress diagrams in Figure 9 The oblong shaped loading areas, which contained about 64 sq in. were made similar to the area of contact between an 8 by 40 in pneumatic tire and a flat surface with the tire inflated to 110 lb per sq in and supporting a 6,000 lb load From Figure 9 it may be noted that in this slab as in No 4 there is a considerable area over which the stress does not vary greatly.

The stresses in slabs 3 and 4 caused by the same magnitude and position of load, and with the load distributed over the same area, may be compared by reference to Figure 9 (a) and Figure 5 Although the slabs were the same thickness and approximately the same size, the maximum stress in slab 3 was only about 55 percent of that in slab 4 This difference is probably attributable to the fact that the subgrade under slab 3 was stiffer than that under slab 4, and that the modulus of elasticity of the concrete in slab 3 was less than that in slab 4 It is difficult, however, to thus account for such a wide divergence in stress, since published analyses of stresses (9) (8) (6) indicate that large variations in either or both of these properties cause relatively little variation in stress

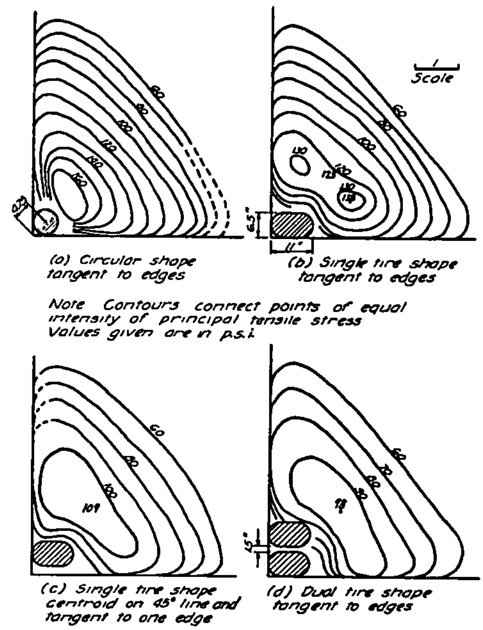

Figure 9 Iso-Stress Diagram for Various Loading Shapes Slab No 3, 5,000-Lb Load

SUBGRADE PRESSURES AND SLAB DEFLECTIONS—SLAB NO 4

As previously mentioned, Goldbeck pressure cells were used to measure subgrade pressures Experience on Slab No 3 had shown that a vertical adjustment of the cell was necessary after the cell was in place in the slab A cross-section of this adjustment device and the cell is shown in Figure 10 An outer casing consisting of the cast iron shell A and the $\frac{3}{8}$ in pipe B enclosed the pressure cell C and its connecting pipe This outer casing was held rigidly in place by the bond between it and the concrete of the slab The cell could be raised a small amount by simply pulling up on the small inner pipe, and could be moved down and held down by screwing the cap D against the shoulder on the inner pipe Thus an initial pressure reading was assured, and moreover it could be adjusted to any desired value within certain limits A circular piece of rubber $\frac{1}{16}$ in thick was cemented to the bottom of the cast iron shell to keep out dirt, and to protect the brass covering G

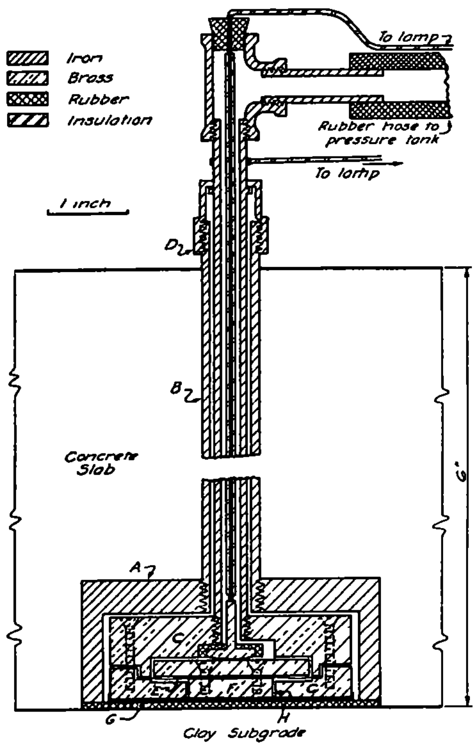

Figure 10 Pressure Cell Adjustment Device

When the cells were originally calibrated it was found that they were not consistent and that the electrical contact was broken at a value of internal pressure which was only about one-fourth of the applied external pressure. This was especially objectionable since it was anticipated that the subgrade pressures would be comparatively small, and with one lb. per sq. in. pressure on the slab being registered as only about one-fourth lb. per sq. in. on the manometer there would not be sufficient accuracy.

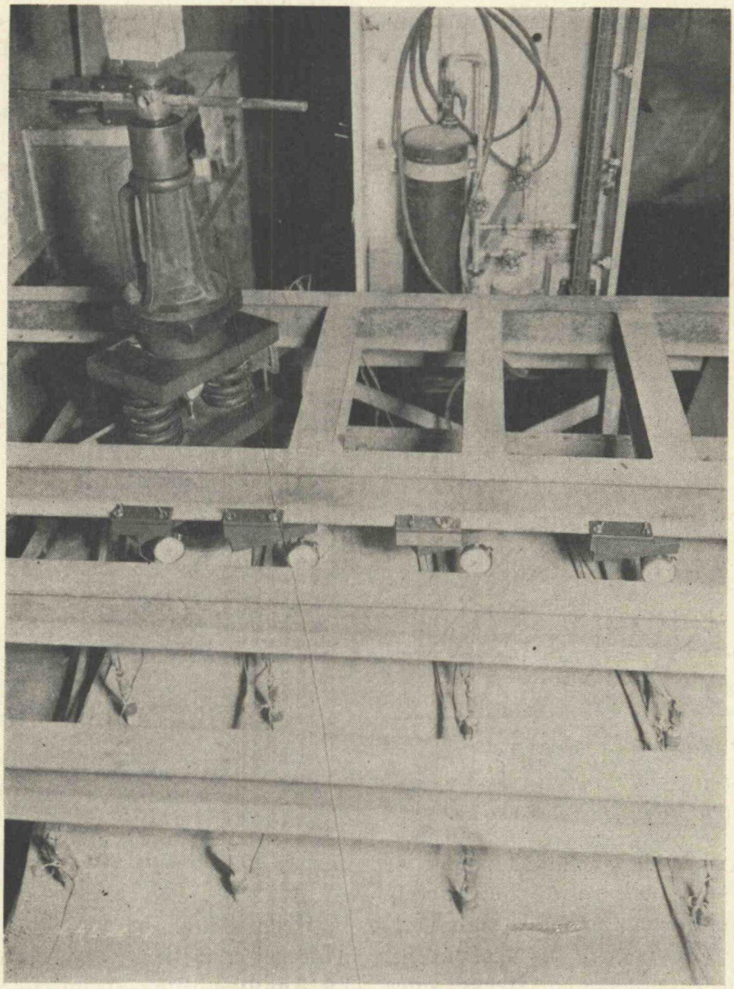

Figure 11. Apparatus for Measuring Subgrade Pressures and Framework Supporting Deflection Dials at N. W. Corner of Slab No. 4.

After considerable study and experimentation it was found that the reason the cells would not calibrate one for one was that the diaphragm E which completely sealed the air pressure from the lower part was tightly pressed against the lower shoulder, and hence could only bend over the narrow width H. Whereas the internal pressure should be acting over an area equal to that of the plunger F, it was acting over this area plus the area of the diaphragm which pulled the lower portion down, breaking the electrical contact long before the internal pressure was equal to the external pressure. If the diaphragm had had no rigidity or had been allowed to bend over a greater width it would have been pressed down on the shoulder without carrying the contact with it.

In order to eliminate this difficulty, a couple of $\frac{1}{8}$ in. holes were punched in the diaphragm E, and the thin brass covering G made air tight. The diaphragm E then had equal air pressure on both sides and could bend over its entire width. Since the external pressure against the plunger F sealed the bottom of it from the internal pressure, the external pressure and the internal pressure now acted over the same areas, and the cells calibrated one for one.

In actual use in the slab a separate hose and electrical circuit were carried from each cell and rigidly fixed to a panel where the electrical and air hose connections were made at the time the cells were read. Some idea of the arrangement may be obtained from Figure 11. Air pressure was supplied from the pressure storage tank and the pressure at the time the electrical contact was broken was measured by a mercury manometer calibrated in ounces. The location of the cells in the slab is shown in Figure 12. The numbers by the cells will be used subsequently to designate a given position on the slab.

Since there was always an initial pressure on the cells, they obviously recorded change in pressure due to the applied load and not absolute pressure. A preliminary study was made to determine what effect various values of this initial pressure, when the slab was unloaded, had on the change in subgrade pressure recorded when the slab was loaded.

It was found that as the initial pressure was increased, the change in pressure due to a given load was also increased although not in direct proportion. This was especially true of the cells located near the corner. Therefore, it was decided that the cells should be adjusted for an initial pressure equal to that caused by the weight of the slab which was approximately 0.5 lb. per sq. in.

With the cells all set at the above initial pressure, the slab was loaded in increments and the pressures recorded at loads of 3,000, 4,000, and 5,000 lb. The difference between the reading at a given load and the initial value gave the pressure caused by the applied load and will be referred to subsequently as simply the subgrade pressure. The tests showed that this subgrade pressure at any given cell

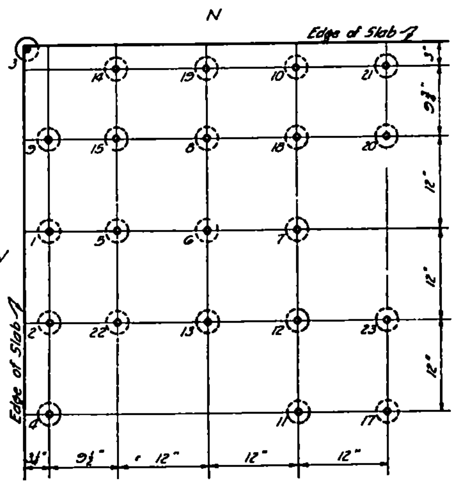

Figure 12. Location of Pressure Cells

varied directly with the applied load. The variation in the pressure for different positions in the slab at a given load is shown in Figure 13. An empirical relationship derived from the experimental data is also shown in the figure

$$p=0.0044P_c\, a^{-0.4}\, e^{-0.07r} \quad \ldots \quad (5)$$

in which

- p = subgrade pressure.
- P_c = load at corner
- a = distance from corner to center of loading area
- e = base of natural logarithms = 2.718
- r = distance from corner to pressure cell

It should not be construed that this equation will give the subgrade pressure on any pavement slab, for it is intended to apply only to the particular slab under investigation here

It can be seen in Figure 13 that for the smaller distances from the corner there are usually two points above the curve and two below it The reason for this is that symmetrically placed cells did not give the same pressure readings, that is, one cell gave high readings and the other one low readings even though they were the same distance from the corner and symmetrically located

The deflections of the slab at each cell position were measured with 0 0001-in Federal dials, which were attached to a steel framework erected to hold the dials rigidly in position A part of this framework may be seen in Figure 11 It consisted of an 18-in I-beam which spanned the slab and was supported on concrete piers. Several 4-in I-beams were bolted between this beam and the concrete basement wall, and the dials fastened to these beams with a special clamp It was necessary to load the slab twice in order to get a complete set of deflection readings, since only ten dials were available

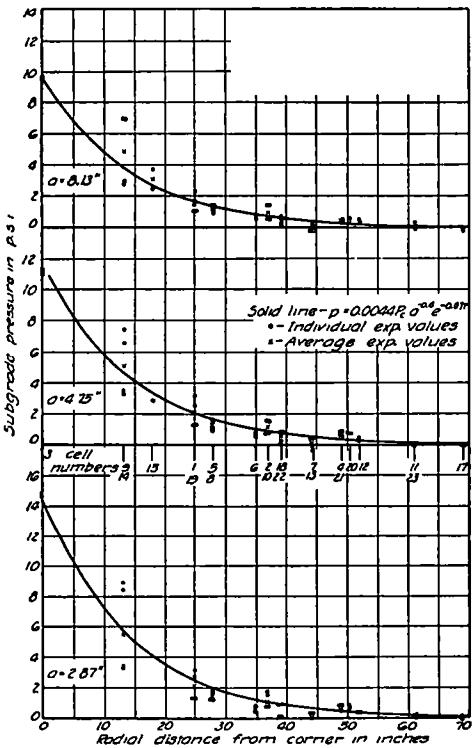

Figure 13 Subgrade Pressures Slab No 4, 5,000-Lb Load

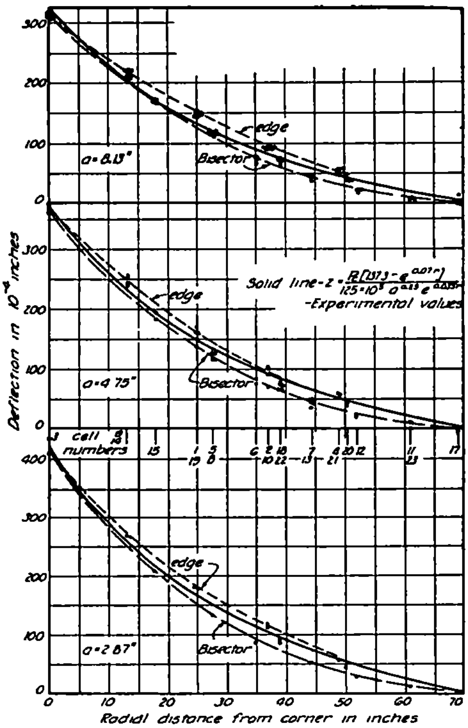

Figure 14 Deflection Curves Slab No 4, 5,000-Lb. Load

As with pressures, it was found that the deflection at a given point varied directly with the applied load The variation in deflection from point to point for a given load is shown in Figure 14 More deflection values are shown than pressure values because deflection readings were taken during the preliminary study of pressures and these have been included. The data show that the deflections along an edge fall on one curve while those along the corner bisector fall on another. However, these curves are not far apart, and the deflections for a given magnitude and position of load approximately follow a curve which depends only on the distance from the corner. An empirical equation,

$$z = \frac{P_c[137.3 - e^{0.07r}]}{125 \times 10^5 a^{0.25} e^{0.035r}} \quad (6)$$

was derived from the experimental deflection data.

The measured deflections show that the slab dishes slightly so that it is concave

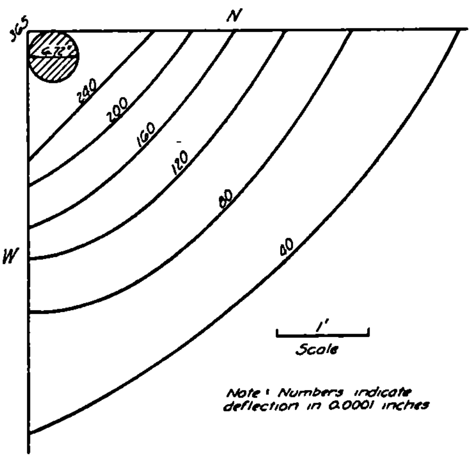

Figure 15. Iso-Deflection Diagram, Slab No. 4, 5,000-Lb. Load

upward as may be seen in the iso-deflection diagram given in Figure 15. This effect increases as the position of the load is moved away from the corner.

Since both the subgrade pressure and the deflection at a given point on the slab varied directly with the load, the ratio of the subgrade pressure to the deflection at a given position is a constant. However, the value of this ratio varies with the distance from the corner. This fact is shown in Figure 16 where the curve is the ratio of the empirical expression for pressure to the empirical expression for deflection. The ratios of the average of the subgrade pressure readings to the average of the deflection readings at corresponding points give quite a scattered set of values especially at the larger distances from the corner where both the pressure and deflection readings were small. The pressure readings in this region were probably less than the precision limits of the pressure cells.

Goldbeck's (1) tests on the effect of size of bearing area on the supporting

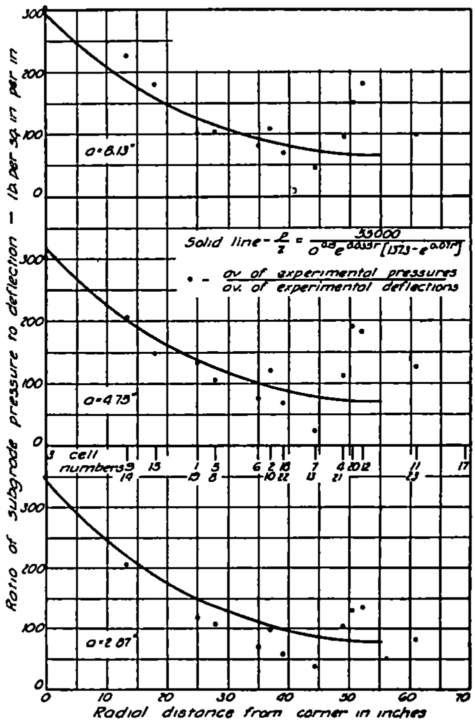

Figure 16. Ratio of Subgrade Pressure to Deflection. Slab No. 4

value of soils show that the ratio of the pressure to the deflection varies approximately inversely as the square root of the area. If the slab is thought of as being broken up into narrow areas perpendicular to the corner bisector, approximately the same relationship exists between these areas and the ratio of subgrade pressure to deflection as Goldbeck observed in his tests. Westergaard (8) called this ratio of subgrade pressure to deflection the "modulus of subgrade reaction," and in his analytical solution assumed it to be a constant of the same value for every point within the area considered Nevertheless, he recognized that it might vary from point to point in the slab, and showed that different values of the ratio in his equations did not materially affect the value of the stress

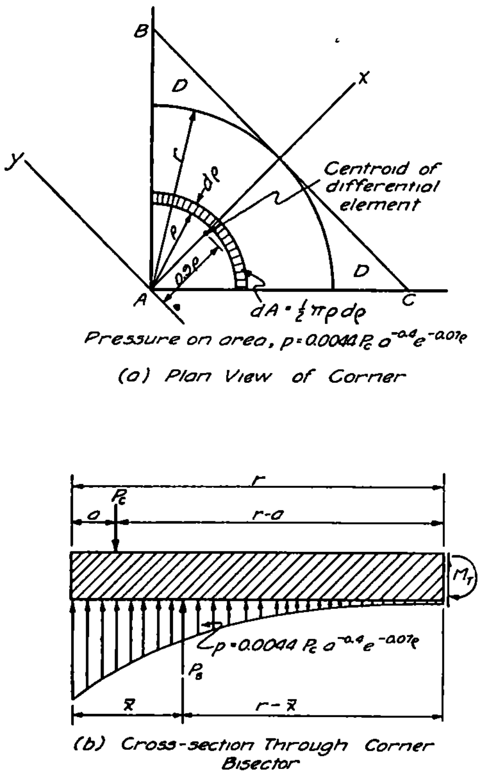

(a) Plan View of Corner

(b) Cross-section Through Corner Bisector

Figure 17

STRESS CALCULATION FROM MEASURED PRESSURE

If the magnitude and position of the centroid of the total subgrade pressure acting on a triangular section of the slab such as the area ABC in (a) Figure 17 could be determined, all of the external forces acting on the section would be known With the forces known, the external bending moment on the section could be found and the average normal stress over the length BC calculated In order to get the total subgrade pressure, the character of the pressure variation over the area must be known The empirical expression for the subgrade pressure gives this variation for this slab

An attempt was made to integrate the subgrade pressure over a triangular area, but the expression encountered could not be integrated Therefore, it was decided to integrate over a circular sector and try to determine the error introduced A conservative estimate indicated that this error was less than one percent

Referring to Figure 17(a) it can be seen that the total subgrade pressure P_s acting on any given circular sector, may be expressed by

$$P_s = \int p\,dA = 0\,0022\pi P_c a^{-0\,4}\int_0^r \rho e^{-0\,07\rho}d\rho = 0\,099P_c a^{-0\,4}[14\,3 - 14\,3e^{-0\,07r} - re^{-0\,07r}] \quad (7)$$

To get the position of P_s, its moment with respect to the y-axis may be determined

$$\begin{aligned} M_y &= 0\,9\int \rho p\,dA = 0\,00198\pi P_c a^{-0\,4}\int_0^r \rho^2 e^{-0\,07\rho}d\rho \\ &= 0\,0888P_c a^{-0\,4}[408 - 408e^{-0\,07r} - 28\,6re^{-0\,07r} - r^2e^{-0\,07r}] \quad . \end{aligned} \quad (8)$$

The distance from the corner to P_s is

$$\bar{x} = \frac{M_y}{P_s} = \frac{0\,897[408 - 408e^{-0\,07r} - 28\,6re^{-0\,07r} - r^2e^{-0\,07r}]}{14\,3 - 14\,3e^{-0\,07r} - re^{-0\,07r}} \quad (9)$$

From the free-body diagram in Figure 17(b) the total external bending moment, M_T, may be obtained

$$M_T = P_c(r - a) - P_s(r - \bar{x}) \quad (10)$$

Substituting the values of P_s and $\bar{x}$ from equations 7 and 9 gives

$$M_T = P_c(r-a) + 0.099P_c a^{-0.4}[367 - 14.3r - 367e^{-0.07r} - 11.4re^{-0.07r} + 0.1r^2e^{-0.07r}] \quad (11)$$

If the total moment M_T is divided by 2r, the width of the section BC, the average moment per unit of width, M_u, is obtained

$$M_u = \frac{P_c}{2}\left(1 - \frac{a}{r}\right) + 0.0495P_c a^{-0.4}\left[\frac{367}{r} - 14.3 - \frac{367}{r}e^{-0.07r} - 11.4e^{-0.07r} + 0.1re^{-0.07r}\right] \quad (12)$$

The average normal stress may now be calculated from the flexure formula,

$$\sigma_n = \frac{6M_u}{h^2} \quad (13)$$

Substituting the value of M_u from equation 12,

$$\sigma_n = \frac{3P_c}{h^2}\left(1 - \frac{a}{r}\right) + \frac{0.296P_c}{h^2a^{0.4}}\left[\frac{367}{r} - 14.3 - \frac{367}{r}e^{-0.07r} - 11.4e^{-0.07r} + 0.1re^{-0.07r}\right] \quad (14)$$

The above expression for σ_n is an unwieldy one, and can best be interpreted from a graph of the equation. The curves showing how this average normal stress, σ_n, varies with the distance from the corner and also with the distance, a, are given in Figure 18 (a). It is interesting to note that as the distance, a, increases, the curves flatten out, and for a = 8.13 in there is a large distance over which the stress is almost constant.

It may be recalled from the previous discussion on average normal stress that to obtain the maximum principal stress from the average normal stress approximately 15 percent should be added to the latter. Figure 18 (b) shows the average normal stress curve for a = 4.75 in with 15 percent added to it and represents approximately the maximum principal stress. The plotted points are the maximum principal stress as determined from the rosette strain readings on another corner of the same slab. The calculations from the empirical equation for pressure give stresses which are fairly consistent with the principal stresses obtained from the rosette strain readings, and it seems should lend a certain amount of confidence to the subgrade pressure measurements.

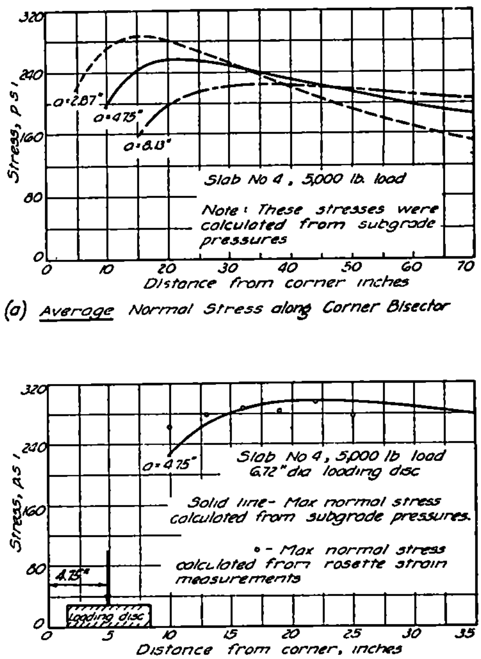

(a) Average Normal Stress along Corner Bisector

(b) Maximum Normal Stress along Corner Bisector

Figure 18

CONCLUSIONS

The foregoing data and calculations which are applicable to the two plain concrete slabs of uniform thickness, supported on a clay subgrade, and loaded at a corner, lead to the following conclusions in regard to these slabs

1 Normal stresses were not uniformly distributed over lines perpendicular to the corner bisector, but were 33 to 45 percent less at the edges than at the bisector Principal stresses at points on these lines were 20 to 40 percent less at the edges than at the bisector

2 There was a comparatively large area in the region of the corner over which the magnitude of the principal stress did not vary greatly

3 The maximum stress in the slab was not materially affected by the area over which the load was distributed, but increased as the centroid of the loaded area approached the corner

5 Apparent stresses were approximately 15 percent greater than the principal stresses in the vicinity of the maximum stress in the slab

6 The ratio of subgrade reaction pressure to deflection was a constant at a given point in the slab, but it varied with the distance of the point from the corner. However, this fact does not seem to affect the stresses computed from the formulas in which it is assumed that the ratio is a constant of the same value at all points

REFERENCES

1 Goldbeck, A T, and M J Bussard "The Supporting Value of Soil as Influenced by the Bearing Area" *Public Roads,* January 1925

2 Hitchcock, W E "Stresses at a Corner of a Concrete Pavement Slab Under Concentrated Loading" Unpublished thesis Library, Iowa State College, Ames, Iowa 1937

3 Lightburn, Frank E "An Investigation of the Plaster Model of Stress Determination and Its Application to Slabs on an Elastic Foundation" Unpublished thesis, Library, Iowa State College, Ames, Iowa 1935

4 Murphy, Glenn "Stresses and Deflections in Loaded Rectangular Plates on Elastic Foundations" Bulletin 135, Iowa Engineering Experiment Station, Iowa State College, Ames, Iowa 1937

5 Osgood, W R, and R G Sturm "The Determination of Stresses from Strains on Three Intersecting Gage Lines and Its Application to Actual Test" *U S Bureau of Standards Journal of Research,* 10 685 1933

6 Spangler, M G "Stresses in Concrete Pavement Slabs" *Proceedings* Highway Research Board, 15 122 1935

7 Timoshenko and MacCullough "Elements of Strength of Materials" p 33 and 46 D Van Nostrand Co, Inc, New York 1935

8 Westergaard, H M "Computation of Stresses in Concrete Roads" *Proceedings* Highway Research Board, 5 91-112, 1926

9 Westergaard, H M "What is Known of Stresses" *Engineering News Record,* 118 26, Jan 7, 1937

DISCUSSION ON CONCRETE PAVEMENT STRESSES

DR RUDOLF K BERNHARD, *Consulting Engineer, Baldwin-Southwark Corporation, Philadelphia* This discussion relates to stresses in concrete pavement slabs induced by *dynamic* loads in contrast to the discussion by Spangler and Lightburn of stresses induced by *static* loads The main purpose of the test reported herein was to determine whether the new method with "induced" vibrations, which has been successfully used for soil tests, can be applied to the investigation of stresses in concrete slabs

Tests were made on a concrete highway which served to answer affirmatively the following questions

1 Will the test indicate the relative rigidities of concrete pavement slabs of different thicknesses laid on a uniform subgrade?

2 Does the area over which the force is applied have any influence in the case of a concrete slab?

A description of the technic of the

dynamic tests was given at the December, 1936, meeting of the Highway Research Board.[1]

The fundamental principle is very simple. A highway under investigation is loaded in various places by alternating forces having a sine form. Frequency and size of these forces can be changed. Hence the slab must vibrate with forced and damped oscillations.

The apparatus for exciting these alternating forces, the "oscillator" is a relatively small machine, which has two discs eccentrically supported. The discs revolve in opposite directions and are rotated by an electric motor. Changing the eccentricity of these discs will change the amount of the centrifugal forces; changing the motor input will change the speed of revolutions, and hence the frequency of the exciting forces. All horizontal forces are neutralized in the body of the machine by the inverse rotation of the two discs. Two external vertical forces alternating in a pure sine form remain. Figure 1 is a picture of the apparatus.

The propagation speed, or phase difference of these induced oscillations, can be determined by measuring with seismometers the phase of two corresponding maxima or minima. The time which is required by the wave to move from a point on or near the oscillator to another point causes a phase difference in both sine curves plotted by the seismometers. By moving the seismometers from point to point, it is possible to record closed profiles or contours with no danger of omitting salient points.

The instruments to record the vibrations consist of two pick-up units to record vertical vibration-amplitudes. Based on the seismic principle their natural frequency is low, approximately only 4 cycles per sec., their damping is carefully controlled to avoid any phase distortion. The recorder is a special com-

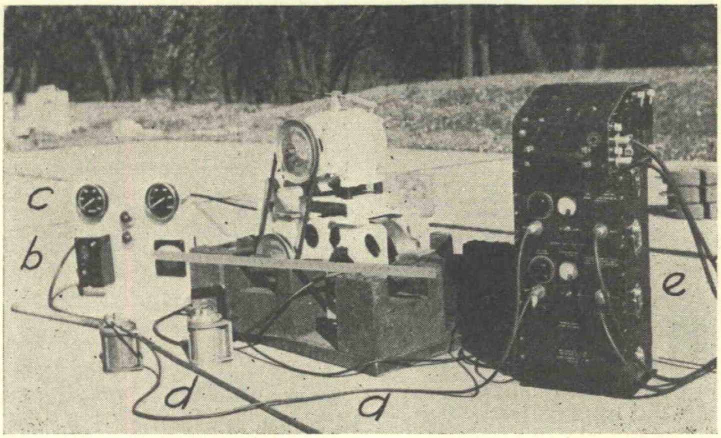

Figure 1

a. Oscillator to Excite Vibrations
b. Switch Board for Oscillator
c. Tachometers to Measure Frequency of Induced Vibrations
d. Pick-Up Units to Measure Vibrations
e. Amplifier and Recorder for Pick-Up Units

[1] *Proceedings,* Highway Research Board, Vol. 16, p. 288 (1936).

pact type of oscıllograph contaınıng two elements wıth a natural frequency of 2500 cycles peı sec An amplıfier unıt enlarged up to 1300 tımes and transformed the voltage ınduced by the two pıck-ups from speed to amplıtude, ı e, ındependent of the frequency wıthın the requıred range Photographıc records can be obtaıned on a standard 16 mıllımeter film wıth a propagatıon speed of 6¼ and 12½ ın per sec respectıvely Hence, two amplıtude measurements can be recorded sımultaneously

TESTS

The total wıdth of the experımental hıghway was 20 ft The dımensıons between the expansıon joınts and outsıde edge of each concrete slab were 10 × 20 ft The thıckness of the slabs varıed from 6 to 9 ın Three dıfferent serıes of ınvestıgatıons were carrıed out

Fırst Serıes The oscıllator was placed near the outer edge of one slab, ın order to have equal dıstance from both longıtudınal and transfer joınts The transfer joınt had a **Y**-shape, the longıtudınal joınt a **U**-shape wıth steel reınforcement The oscıllator excıted centrıfugal forces of ±600 lb (10° eccentrıcıty) at a frequency of 27 cycles per sec, and ±300 lb at 22 cycles per sec The first pıck-up was moved from a poınt near the oscıllator ın steps to a maxımum dıstance of 100 ft The maxımum sensıtıvıty was, however, not reached ın thıs dıstance The second pıck-up remaıned always at the first poınt as reference and control

The densıty of the soıl has not been substantıally ımproved by the concrete pavement Both slab and soıl vıbrate almost as a unıt and no slıdıng motıon wıll occur between the adjacent surface Hence, the slab should be made only strong enough to resıst local stresses by outsıde loads (vehıcles) The relatıve phase speed ın slabs of dıfferent thıcknesses and the subsoıl thus forms a convenıent means, ın certaın cases, to predetermıne the requıred thıckness of pavements

The hıgh amplıtudes along the free longıtudınal edges of the slabs produce the so-called "flutter effect," whıch ındıcates the ımportance of concrete and steel reınforcement along these edges

Second Serıes The oscıllator was placed ın the center of a 9 ın thıck slab, and the seısmographs moved systematıcally step by step over the complete surface of thıs slab Fıgure 2 represents the maxımum half-amplıtudes ın two ordınates Agaın the contınuıty of the waves near the adjacent joınts and the relatıvely hıgher amplıtudes at the free edges can be clearly recognızed The maxımum stress (7 lb per sq ın) occurs under the excıtıng force, causıng a steep inclıne of amplıtudes ın both ordınates (maxımum amplıtude 0 00086 ın)

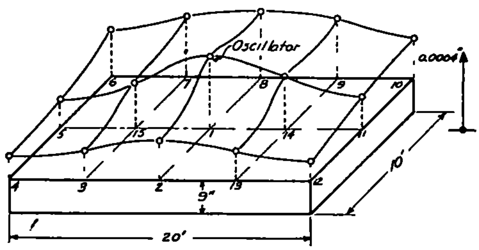

Fıgure 2 Maxımum Deformatıon of 9-In Concrete Slab Under Dynamıc Load ın Center of Plate

Maxımum Excıtıng Force, 600 Lb at 27 Cycles Per Sec

Maxımum Half-Amplıtude, 0 00043 In

Maxımum Stress at Poınt I, 7 Lb Per Sq In

Thırd Serıes The same ınvestıgatıon as descrıbed under Serıes Two was repeated on a 6-ın slab Fıgure 3 shows the maxımum half-amplıtude ın two ordınates The same phenomena as ın Serıes Two can be observed The maxımum amplıtude has ıncreased to 0 0022 ın (1 2 5) The peak stress has been determıned at 12 lb per sq ın

The pronounced hump which is also clearly to be seen in the two figures has increased in Figure 3 which indicates obviously the varying rigidity of the slabs or in other words the influence of the thickness of the slabs, including the effect of the subsoil

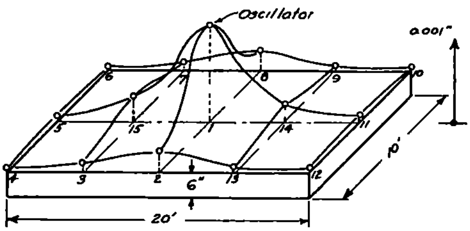

Figure 3 Maximum Deformation of 6-In Concrete Slab Under Dynamic Load in Center of Plate

Maximum Exciting Force, 600 Lb at 27 Cycles Per Sec

Maximum Half-Amplitude, 0 0011 In

Maximum Stress at Point I, 12 lb Per Sq In.

Furthermore, the conclusion might be drawn that a broader distribution of the applied load will flatten substantially the height of this hump and reduce the local stresses

MR R D BRADBURY, *Wire Reinforcement Institute* The results disclosed by this experimental investigation indicate that the actual maximum intensity of stress is slightly greater than that computed by the formula for corner loading in accordance with Westergaard's theoretical analysis Apparently this discrepancy is largely attributable to the fact that the intensity of observed stress is not uniformly distributed on a straight-line section across the slab corner as is assumed by Westergaard But it is possible that, under actual road conditions, other factors may be involved, such as the subgrade, which might not always act in the ideal manner assumed in the theoretical analysis

For example, Spangler,[1] in his preliminary investigations, found evidence of a decrease in effective subgrade pressure after a corner load had been repeated several times As stated by Spangler, this suggested the possibility of a slight permanent compaction of the subgrade in the vicinity of the corner as a result of repeated loading If such a condition tends to develop in practice, then it is reasonable to conclude that the virtual subgrade modulus which is effective for the corner segment as a whole might be materially less than the normal modulus as based upon continuous initial contact between the slab and the subgrade Of course, any attempt to evaluate a condition of this kind necessarily requires a purely arbitrary assumption as to the amount of reduction to be applied to the normal subgrade modulus But the influence of the subgrade is such that a rather wide range in the value of the subgrade modulus has a relatively minor effect upon the intensity of computed stress

According to Westergaard's analysis the value of the radius of relative stiffness of slab to subgrade, l, varies inversely as the fourth root of the subgrade modulus, k If, in arbitrarily fixing the effective value of k for the corner, one assumes for example that its value is only $\frac{1}{4}$ of the normal modulus, then the stiffness radius applicable to the case of corner loading would become $l\sqrt[4]{4}=l\sqrt{2}$

The Westergaard formula[2] for maximum stress under corner loading is,

$$S=\frac{3P}{h^2}\left[1-\left(\frac{a\sqrt{2}}{l}\right)^{0\ 6}\right]$$

If, according to the above assumption, $l\sqrt{2}$ is substituted for l, one would obtain a modified corner formula,

$$S=\frac{3P}{h^2}\left[1-\left(\frac{a}{l}\right)^{0\ 6}\right]$$

[1] See *Proceedings*, Highway Research Board, Vol 15, p 122

[2] See *Proceedings*, Highway Research Board, Vol 5, p 90

According to the paper, the general test conditions applying to Slab No 4 were,

$$
\begin{aligned}
E &= 4{,}000{,}000 \text{ lb per sq in} \\
u &= 0\ 25 \\
a &= 3\ 36 \text{ in} \\
P &= 5{,}000 \text{ lb} \\
k &= 200 \text{ lb per in}^{3} \\
h &= 6 \text{ in}
\end{aligned}
$$

from which the computed radius is $l = 24\ 9$ in Applying the above modified formula, the computed maximum stress is,

$$S = \frac{3 \times 5000}{6 \times 6}\left[1 - \left(\frac{3\ 36}{24\ 9}\right)^{0\ 6}\right]$$

$$= 292 \text{ lb per sq in}$$

which corresponds very closely with the observed maximum principal stress of 294 lb per sq in on the corner bisector as shown in the authors' Figure 4

Subsequent tests with different conditions may, of course, fail to exhibit as close a check with the modified formula as is obtained for this specific case But, until valid relationships are revealed by further investigations, it would seem not only desirable but entirely permissible, for practical purposes of stress computation, to make use of some such modification of the Westergaard formula—a formula which is both plausible and consistent in general form and which has the commendable feature of algebraic simplicity